*J. Univ. Kuwait (Sci.)* **13**, 1986

# Impact of refinements of photo coordinates on accuracy of single photo resection and orientation

MOHAMED S. ELGHAZALI AND ASHRAF N. SAYED

*Departments of Civil Engineering, University of Kuwait, P.O. Box 5969, Kuwait and Faculty of Engineering, Cairo University, Giza, Cairo, Egypt*

## ABSTRACT

In photogrammetry, the concept of collinearity is based on the assumption that the object space point, the exposure station and the image space point lie on a common straight line. In practice, however, this line deviates from straightness due to different linear and nonlinear systematic errors, thus affecting the location of images on the photograph. This paper studies the effect of some important sources of error on the determination of parameters of single photo resection and orientation. By applying corrections to the photo coordinates, the mean values of the observational residuals (after a least squares adjustment) improved from 8 $\mu$m to 6 $\mu$m at photo scales. It has also been shown that both atmospheric refraction and earth curvature corrections should be either applied or ignored because of their compensating effect. Correcting for either of them alone causes deterioration in accuracy when determining the parameters.

## 1. INTRODUCTION

One of the classification schemes of photogrammetry is based on the way of solving the projective transformation between photo and ground coordinates. Generally, we have two main approaches, namely: analogue photogrammetry and analytical photogrammetry.

Traditionally, photogrammetry was developed along the analogical line where a situation similar to that prevailing during the taking of the photograph was created in the laboratory. This approach requires the use of special restitution instruments, which are among the main sources of errors due to imperfections in their optical mechanical components, and their inability to accurately compensate for systematic errors.

Analytical photogrammetry employs mathematical equations in dealing with the problem and the collinearity condition is the fundamental relationship. Under operational conditions, systematic errors cause disturbances to the idealised concept of collinearity. One main advantage of analytical photogrammetry over analogue photogrammetry lies in the fact that it allows—by imposing corrections—the elimination of some of these errors. In theory, there are no limitations as to how far we can correct

for error sources. In practice, however, we are limited by the rigor of the mathematical modelling of the errors and our lack of knowledge of all error sources. In this regard, five most common errors occurring during the photographing process are considered. These are lack of coincidence between principal point and fiducial centre, shrinkage or expansion of photographic material, radial lens distortion, atmospheric refraction and earth curvature (Wolf 1983). The effect of refining photo coordinates from these errors on the accuracy of the solution of single photo resection and orientation is studied. Resection involves the computation of the positional coordinates of the exposure station ($X_0$, $Y_0$, $Z_0$), while orientation leads to the computation of the angular relationships ($\omega$, $\phi$, $\kappa$) between the survey and photographic coordinate systems. Modern computational procedures compute both resection and orientation simultaneously as will be illustrated in the present paper.

## 2. MATHEMATICAL MODELS

### 2.1. COLLINEARITY CONDITION

The concept of collinearity for a vertical photograph is defined with reference to Fig. 1, where the object space point ($A$), the exposure point ($O$) and the image space point ($a$) lie on a common line. The result of the collinearity assumption is the establishment of similar triangles between corresponding image and object space points. For tilted photographs, the image space must first be transformed parallel to the object space. From these similar triangles, it is seen that

$$\left.\begin{aligned} x_a &= \frac{C}{Z_A} \cdot X_A \\ y_a &= \frac{C}{Z_A} \cdot Y_A \end{aligned}\right\} \qquad (1)$$

This is an important result which is used to develop the projective equations for the general case of tilted photographs used for the determination of single photo resection and orientation parameters.

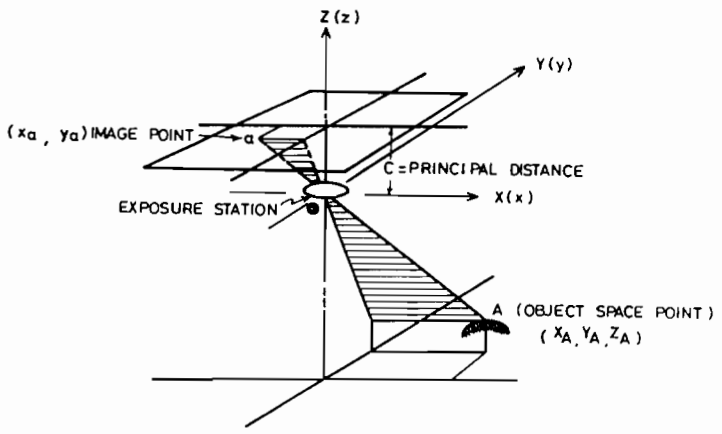


**Fig. 1.** The collinearity concept (after Merchant 1973).

## 2.2. REFINEMENTS OF PHOTO COORDINATES

### *2.2.1. Lack of coincidence between principal point and fiducial centre*

This is a linear error that can be corrected by two shifts in both $x$ and $y$ directions. For any image point, reduction from fiducial axes to principal axes is given by

$$\left.\begin{aligned} x_1 &= x - x_0 \\ y_1 &= y - y_0 \end{aligned}\right\} \tag{2}$$

where

$(x, y)$ are the photo coordinates with respect to the fiducial system,
$(x_1, y_1)$ are the photo coordinates with respect to the principal point system, and
$(x_0, y_0)$ are the coordinates of the principal point with respect to the fiducial system.

### *2.2.2. Shrinkage or expansion of photographic film*

Dimensional instability of films is mainly due to temperature changes, humidity changes, variation in tension and aging. The consequence is a non-linear film deformation that can only be corrected using reseau photography. Since the photographs used in this study have only side fiducial marks, the linear part of this error is corrected based on

$$\left.\begin{aligned} x_2 &= (x_c/x_m) \cdot x_1 \\ y_2 &= (y_c/y_m) \cdot y_1 \end{aligned}\right\} \tag{3}$$

where

$(x_2, y_2)$ are the photo coordinates after second correction,
$(x_m, y_m)$ are the measured fiducial distances between opposite fiducial marks, and
$(x_c, y_c)$ are the corresponding calibrated fiducial distances.

### *2.2.3. Objective lens distortion correction*

One definition of distortion is in terms of the lack of constant image magnification within the adopted plane of focus. In photogrammetry, since we are invariably working with image coordinates $(x, y)$, it is more convenient to consider distortion as a disturbance in terms of image coordinates rather than a variation in camera constant from point to point. In the present study, the radial lens distortion was corrected for each point based on its position within the photograph and the lens calibration curve. The tangential lens distortion, being the smaller distortion component, is usually ignored (Merchant 1973). Three different methods of correcting lens distortion are being alternatively applied in practice: (a) reading the required corrections from a radial lens distortion curve, (b) interpolating corrections from a table, and (c) using numerical methods in which the radial lens distortion curve is approximated by a polynomial. In this investigation the first method has been applied, where the radial distance $(r)$ from the principal point to each point $(x, y)$ has been computed from

$$r = \sqrt{x_2^2 + y_2^2} \quad . \tag{4}$$

Then the correction of the radial lens distortion from the corresponding distortion

curve is obtained and is denoted by ($\Delta r$). The corrected radial distance ($r_1$) for each point is given by Eq. 5, keeping in mind that $\Delta r$ could be either positive or negative.

$$r_1 = r + \Delta r \quad . \tag{5}$$

This error is non-linear and its effect is corrected according to Eqs 6 resulting in photo coordinates ($x_3$, $y_3$) corrected for previous sources of error and radial lens distortion,

$$\left.\begin{aligned} x_3 &= (r_1/r) \cdot x_2 \\ y_3 &= (r_1/r) \cdot y_2 \quad . \end{aligned}\right\} \tag{6}$$

### *2.2.4. Atmospheric refraction correction*

Due to differences in densities between layers of the atmosphere, light rays do not travel in straight lines (Fig. 2). This source of error causes all imaged points to be displaced outward from the corresponding positions by a distance $\delta r$. Assuming that the atmosphere conforms to the Air Research and Development Command (ARDC) of the U.S. Air Force Model Atmosphere, the value of $\delta r$ can then be computed by Expression 7 (Merchant 1973; Moffitt & Mikhail 1980).

$$\delta r = K\left(r_1 + \frac{r_1^3}{f^2}\right) \tag{7}$$

in which, by the ARDC model, $K$ is a constant given by

$$K = \left[\frac{2410H}{H^2 - 6H + 250} - \frac{2410}{h^2 - 6h + 250}\left(\frac{h}{H}\right)\right] \cdot 10^{-6} \tag{8}$$

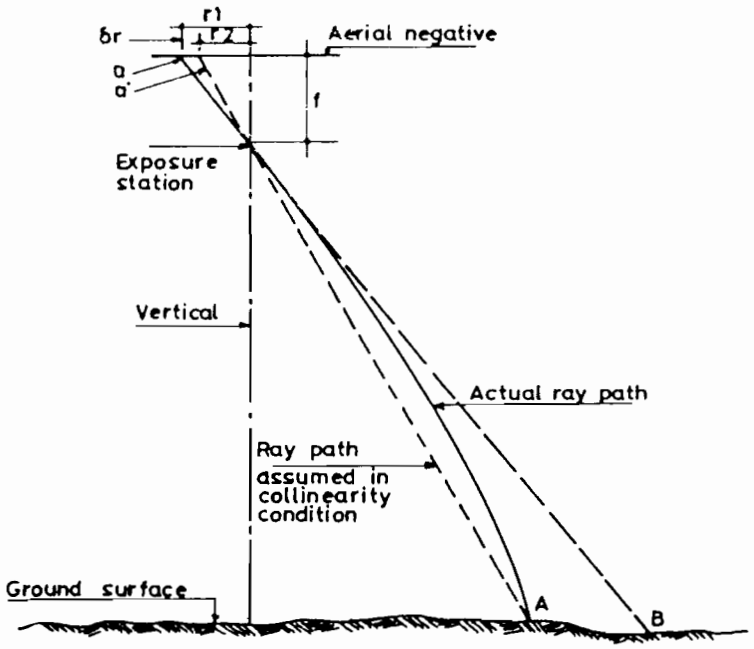


**Fig. 2.** Error caused by atmospheric refraction ($\delta r$) (after Wolf 1983).

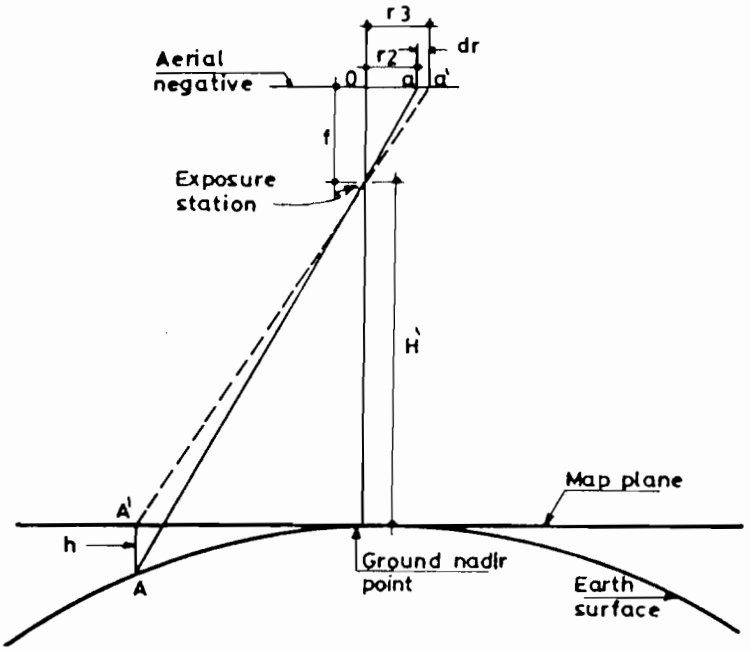


**Fig. 3.** Displacement due to earth curvature (*dr*) (after Wolf 1983).

where

$f$ is the camera focal length,
$H$ is the elevation of exposure station above datum in (km), and
$h$ is the elevation of the point above datum in (km).

Then, the corrected radial distance ($r_2$) is given by

$$r_2 = r_1 - \partial r \quad . \tag{9}$$

Accordingly, the photo coordinates ($x_4$, $y_4$) corrected for previous sources of errors and atmospheric refraction are given by

$$\left.\begin{aligned} x_4 &= (r_2/r_1) \cdot x_3 \\ y_4 &= (r_2/r_1) \cdot y_3 \end{aligned}\right\} \tag{10}$$

*2.2.5. Earth curvature correction*

This error results from the fact that positions of points in the object space are computed in a plane coordinate system. Since the map position $A'$ (Fig. 3) is desired in computation, it is necessary to use the photo coordinates of the theoretical image position $a'$ instead of the actual image position $a$. Distance $aa'$ ($dr$), is the displacement due to earth curvature and is given by Eq. 11 (Wolf 1983).

$$dr = \frac{H' r_2^3}{2Rf^2} \tag{11}$$

where

$H'$ is the flying height above ground, and $R$ is the earth's radius.

Unlike the atmospheric refraction, this error is always applied outward. Therefore, the corrected radial distance ($r_3$) is given by

$$r_3 = r_2 + dr \quad . \tag{12}$$

The final corrected photo coordinates ($x_5$, $y_5$) from all five sources of errors are then given by

$$\left.\begin{aligned} x_5 &= (r_3/r_2) \cdot x_4 \\ y_5 &= (r_3/r_2) \cdot y_4 \quad . \end{aligned}\right\} \tag{13}$$

### 2.3. PROJECTIVE EQUATIONS FOR SINGLE PHOTO RESECTION AND ORIENTATION

The gimbal form of projective equations is currently preferred due to its utility for applications. These equations represent the backbone of analytical photogrammetry and they relate photo coordinates ($x$, $y$) and survey coordinates ($X$, $Y$, $Z$) to elements of exterior orientation ($\omega$, $\phi$, $\kappa$, $X_0$, $Y_0$, $Z_0$). These are expressed by Eqs 14, where ($C$) is the camera principal distance (Merchant 1973).

$$x - x_0 = \\ = c \cdot \left[ \frac{(X - X_0)\cos\phi\cos\kappa + (Y - Y_0)(\cos\omega\sin\kappa + \sin\omega\sin\phi\cos\kappa) + (Z - Z_0)(\sin\omega\sin\kappa - \cos\omega\sin\phi\cos\kappa}{(X - X_0)\sin\phi - (Y - Y_0)\sin\omega\cos\phi + (Z - Z_0)\cos\omega\cos\phi} \right]$$

$$y - y_0 = \\ = c \cdot \left[ \frac{-(X - X_0)\cos\phi\sin\kappa + (Y - Y_0)(\cos\omega\cos\kappa - \sin\omega\sin\phi\sin\kappa) + (Z - Z_0)(\sin\omega\cos\kappa + \cos\omega\sin\phi\sin\kappa}{(X - X_0)\sin\phi - (Y - Y_0)\sin\omega\cos\phi + (Z - Z_0)\cos\omega\cos\phi} \right] . \tag{14}$$

These equations may be concisely expressed in a form more suitable for subsequent adjustment computational procedures as

$$\left.\begin{aligned} F(x) = 0 &= (x - x_0) - C \cdot \frac{\Delta X}{\Delta Z} \\ F(y) = 0 &= (y - y_0) - C \cdot \frac{\Delta Y}{\Delta Z} \quad . \end{aligned}\right\} \tag{15}$$

## 3. PRACTICAL EXPERIMENTATION

### 3.1. DATA ACQUISITION

Photography of a region at Abou Tartour in Egypt, taken with a camera of the following characteristics was used for the present study:

Model: Zeiss RMK A 15/23, No. 21217; Lens: Pleogon No. 98181, maximum aperture F/5·6, nominal focal length 153 mm.

Laboratory calibration report of the camera, using the multicollimator method gave a value of 152·66 ± 0·01 mm as the calibrated focal length (CFL). The radial distortion curves for the camera objective lens are shown graphically in Figs 4 and 5 for the sides and diagonals respectively. Also the coordinates of the fiducial marks of the camera are given in Table 1.

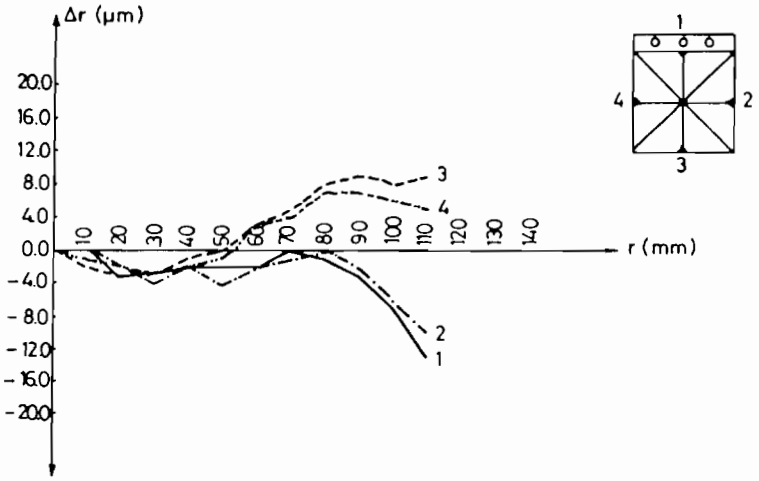


**Fig. 4.** Radial distortion curves in sides 1, 2, 3 & 4.

It is obvious that these data were essential for correcting the photo coordinates for subsequent determination of single photo resection and orientation parameters. A Kern MK2 monocomparator (accuracy 1 $\mu$m) was used for measuring photo coordinates. This comparator is designed in such a way that there is no mechanical contact between the glass scale and the encoder head. The scales are placed as closely as possible in the plane of the diapositive, thereby very nearly fulfilling the Abbe principle.

### 3.2. DATA PROCESSING

Three computer programmes have been developed to process the data (Nasr 1983). These programmes are: (a) affine transformation programme, (b) refinements of photo coordinates programme, and (c) single photo resection and orientation programme.

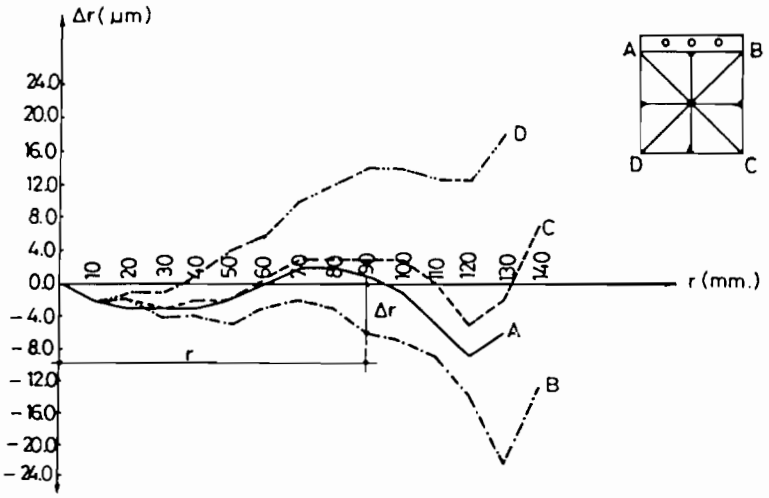


**Fig. 5.** Radial distortion curves in diagonals A, B, C & D.

**Table 1.** Calibrated coordinates of fiducial marks

| Fiducial mark No. | $x$(mm) | $y$(mm) |
|---|---|---|
| 1 | 112·996 | 0·003 |
| 2 | 0·002 | 112·998 |
| 3 | −112·999 | −0·001 |
| 4 | −0·001 | −112·999 |

A six-parameter affine transformation has been used to transform the measured comparator coordinates to the photo coordinates. This transformation allows for a rotation, two translations, two scale changes as well as nonperpendicularity of the comparator axes. The photo coordinates were then corrected sequentially based on Eqs 2, 3, 6, 10 and 13. Finally, the problem of resection and orientation was solved based on Eqs 14 to obtain the six elements of exterior orientation.

A least squares adjustment procedure was used to solve these elements of exterior orientation. However, since the basic mathematical model is non-linear, it was first approximated with a linear function by means of Taylor's series, neglecting second and higher order terms (Mikhail 1976; Merchant 1973; Ghosh 1979). For each observed point ($j$), the observation equations are expressed concisely by

$$A_j \cdot V_j + B_j \cdot \Delta + E_j = \bar{O} \tag{16}$$

where

$A_j$ = partial derivative of Eqs 15 with respect to photo observations $(x_j, y_j)$

$$= \begin{bmatrix} \partial F(x_j)/\partial(x_j, y_j) \\ \partial F(y_j)/\partial(x_j, y_j) \end{bmatrix} = \begin{bmatrix} 1 & 0 \\ 0 & 1 \end{bmatrix} = I$$

$B_j$ = partial derivative of Eqs 15 with respect to unknown parameters

$$= \begin{bmatrix} \partial F(x_j)/\partial(\kappa, \phi, \omega, X_0, Y_0, Z_0) \\ \partial F(y_j)/\partial(\kappa, \phi, \omega, X_0, Y_0, Z_0) \end{bmatrix}$$

$V_j^T$, the residual vector = $[V_{xj}, V_{yj}]$,
$\Delta^T$, the alteration vector = $[\delta\kappa, \delta\phi, \delta\omega, \delta X_0, \delta Y_0, \delta Z_0]$, and

$E_j$, the discrepancy vector = $\begin{bmatrix} F(x_j) \\ F(y_j) \end{bmatrix}$ .

Expanding the observation equations form to include all image points ($j$) observed from 1 to $n$ on a single photo, we have

$$_{2n}[V]_1 + {}_{2n}[B]_6 \cdot {}_6[\Delta]_1 + {}_{2n}[E]_1 = {}_{2n}[\bar{O}]_1 \quad . \tag{17}$$

Then the normal equations are obtained as follows:

$$\underbrace{[B]^T \cdot [W] \cdot [B]}_{[N]} \cdot [\Delta] + \underbrace{[B]^T \cdot [W] \cdot [E]}_{[U]} = [\bar{O}]$$

**Table 2.** Type of correction for different cases
a: No corrections, b: Shrinkage correction, c: Radial lens distortion correction, d: Atmospheric refraction correction, e: Earth curvature correction, ●: Correction has been applied.

| Case | Correction | | | | |
|---|---|---|---|---|---|
| | a | b | c | d | e |
| Case No. 1 | ● | | | | |
| Case No. 2 | | ● | | | |
| Case No. 3 | | ● | ● | | |
| Case No. 4 | | ● | ● | ● | |
| Case No. 5 | | ● | ● | ● | ● |

or more concisely

$$ {}_6[N]_6 \cdot {}_6[\Delta]_1 + {}_6[U]_1 = {}_6[\bar{O}]_1 \tag{18} $$

where

$[N]$ is the normal coefficient matrix,
$[U]$ is a constant vector, and
$[W]$ is the weight matrix of observations.

The weight matrix is taken as the *a priori* estimate of the inverse of the variance–covariance of the observed photo coordinates. Since observations of photo coordinates were made by using a two-axis rectangular coordinate comparator, it is sufficient to assume that $[W]$ is diagonal.

Finally, the solution of the unknown parameters is given by

$$ [\Delta] = -[N]^{-1} \cdot [U] \quad . \tag{19} $$

### 3.3. CASE STUDIES

To test the effect of applying corrections to photo coordinates, five cases have been studied. They are summarized in Table 2. For each of the five cases in Table 2, a number of three or four photographs were used. The results shown later are simply the averages of these photographs for each individual case since they are similar in all geometrical and computational aspects. The approximate photo-scale is 1 : 10 000 which corresponds to a flying height of 1500 m above datum. For each photograph ground control points from accurate ground surveying methods were chosen such that a strong geometry would be achieved. A number of six full ground control points were used for each photograph. They were located close to the four corners in addition to midpoints of 2 opposite sides of the photograph. This distribution ensures large values for the determinates of both the matrices of the observation and the normal equations.

Horizontal control points were established from angular and linear measurements of a traverse meeting the second order accuracy requirements such that the ratio of the closing error to the unadjusted horizontal distance did not exceed 1 in 10 000.

Also, the angular closing error of the unadjusted horizontal angles was less than $10\sqrt{N}$ seconds, where $N$ is the number of traverse sides.

Vertical control was established by a second order levelling procedure with a maximum error of less than $8{\cdot}4\sqrt{K}$ mm, where $K$ is the length of the circuit covered in km.

The area used in this study can be practically classified as flat terrain; its average elevation, based on ground control points, is 217·59 m above M.S.L. with a maximum difference in height of 18·56 m.

## 4. RESULTS AND ANALYSIS

Several computer runs were performed and comparison between the five cases is based on analysis of the variance–covariance matrix of the adjusted parameters and observations. The prime interest was to inspect the improvement or deterioration of the variance of the solved parameters as well as the observational residuals for each case. It was also important to test the validity of the mathematical treatment using Chi-square tests.

The output from each run consists of the residual vector of photo observations ($V$), the variance–covariance matrix of photo observations ($\Sigma L_a$), the alteration vector ($\Delta$), the adjusted vector of parameters ($X_a$), the *a posteriori* variance of unit weight ($\hat{\sigma}_0^2$), the variance–covariance matrix of parameters ($\Sigma \Delta$) and the correlation coefficient matrix of parameters.

The standard deviations of the parameters for the different cases are represented graphically in Figs 6 and 7 for the orientation elements ($\omega$, $\phi$, $\kappa$) and the resection elements ($X_0$, $Y_0$, $Z_0$) respectively.

Figs 6 and 7 show a similar behavioural pattern in the accuracy of the rotational and translational parameters for the different cases. The standard deviations decreased gradually from cases 1 to 3. Then, by correcting for the atmospheric refraction in addition to the first three corrections, the accuracy of the solved para-

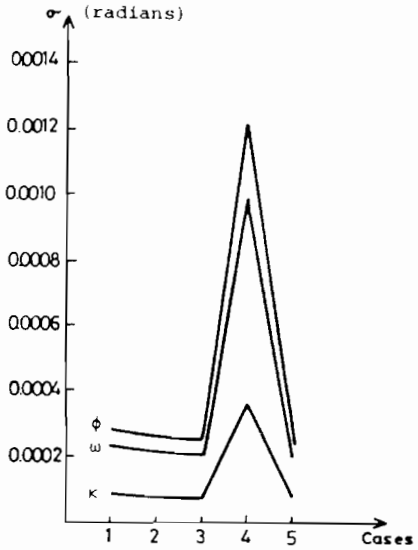


**Fig. 6.** Standard deviations of orientation elements ($\omega$, $\phi$, $\kappa$) for the five cases.

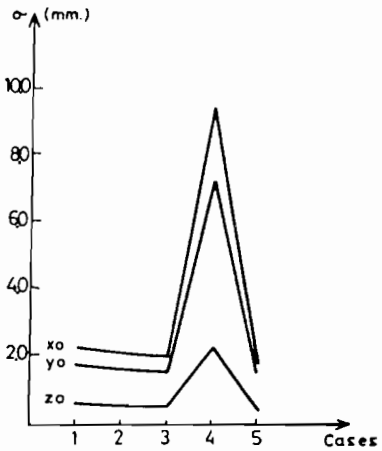


**Fig. 7.** Standard deviations of resection elements ($X_0$, $Y_0$, $Z_0$) for the five cases.

meters dropped significantly. However, this deterioration was over-compensated when the earth curvature correction was considered in case 5. This pronounced change in accuracy from case 4 to case 5 is attributed to the fact that atmospheric refraction and earth curvature always have opposite effects on the position of the imaged points. While the former causes image points to be displaced outward, the latter always acts in a reverse direction displacing image points inward. The magnitude of both errors seems to be of close order under normal physical and geometrical conditions of aerial photography as described earlier.

After the adjustment procedure, the observational residuals ($V$) were computed using

$$V = L_a - L_b \tag{20}$$

where

$L_a$ represents the values of the observations after adjustment, and
$L_b$ represents the values of the observations before adjustment.

The mean values of absolute residuals of photo coordinate observations for the five cases are presented in Table 3.

By sequentially applying the five corrections discussed in (2.2), the overall accuracy of the parameters solution improved by approximately 25%.

Testing the *a priori* variance of unit weight ($\sigma_0^2$) against the *a posteriori* variance of unit weight ($\hat{\sigma}_0^2$), gives an indication of the validity of the adjustment procedure. A Chi-square test ($\chi^2$) for a certain number of degrees of freedom (D.F.) at a significance level ($\alpha$) of 0·05, is expressed by Formula 21 (Hamilton 1964).

**Table 3.** Mean values of absolute residuals from five cases

| Case No. | 1 | 2 | 3 | 4 | 5 |
|---|---|---|---|---|---|
| $\Sigma \lvert V \rvert / n$ (mm) | 0·0084 | 0·0069 | 0·0068 | 0·0398 | 0·0063 |

**Table 4.** Results of testing $\hat{\sigma}_0^2$ versus $\sigma_0^2$ for D.F. = 6 and significance level $\alpha = 0{\cdot}05$

| Case No. | 1 | 2 | 3 | 4 | 5 |
|---|---|---|---|---|---|
| $\hat{\sigma}_0^2$ | 1·351 | 1·179 | 1·081 | 25·109 | 0·990 |
| $\chi^2 = \left(\frac{\hat{\sigma}_0^2}{\sigma_0^2}\right)$ D.F. | 8·108 | 7·073 | 6·483 | 150·660 | 5·941 |
| $\chi^2_{6;0\cdot025}$ | 14·450 | 14·450 | 14·450 | 14·450 | 14·450 |
| $\chi^2_{6,0\cdot975}$ | 1·240 | 1·240 | 1·240 | 1·240 | 1·240 |

$$P(\chi^2_{\text{D.F.},0\cdot025} > \frac{\hat{\sigma}_0^2 \cdot \text{D.F.}}{\sigma_0^2} > \chi^2_{\text{D.F.},0\cdot975}) = 0{\cdot}95 \quad . \tag{21}$$

The result of the test for the five cases is given in Table 4, from which it is seen that cases 1, 2, 3 & 5 passed the test, while the computed $\chi^2$ of case 4 exceeded the upper value of the tabulated $\chi^2$.

It should be clear that the reason case 4 failed to pass the test is due to the detiorating effect resulting in large values for the observational photo residuals ($V$). Accordingly, the value of $\hat{\sigma}_0^2 = V^T WV/\text{D.F.}$ was significantly large and equalled 25·109. The selected value of the *a priori* variance of unit weight does not affect this statistical test because the ratio ($V^T WV/\sigma_0^2$) is invariant with regard to $\sigma_0^2$. Throughout the computations, $\sigma_0^2$ was taken equal to unity.

## 5. CONCLUSION

For precise analytical work, a recent camera calibration report must be available. The calibration parameters are the main source for providing required information for most of the photo coordinate corrections. Results showed an accuracy improvement of approximately 25% by refining the photo coordinates prior to the solution of the resection and orientation parameters. However, it was clear that the effect of atmospheric refraction was compensated to a great extent by earth curvature since their influence on the position of image points is always opposite in direction. Non-linear film deformation can not be described with reference to fiducial marks employed in most of aerial mapping cameras. The use of glass rather than film base will of course eliminate this problem. However, an alternative is offered in recent cameras in which an array of control points (reseau) are imaged at closely spaced intervals at the instant of exposure. The result is sufficient control to recover local film deformation due to shrinkage as well as unflatness.

## ACKNOWLEDGEMENTS

The authors would like to acknowledge the guidance provided by Professor Sabbah, Professor of Surveying and Geodesy at Cairo University. Appreciation is also extended to the Military Survey Department of Egypt for use of their Kern MK2 monocomparator and to the ICL Computer Centre of Cairo University for data processing.

## REFERENCES

**Ghosh, S. 1979.** Analytical photogrammetry. Pergamon Press, New York.

**Hamilton, W. 1964.** Statistics in physical sciences. The Roland Press, New York.

**Merchant, D. 1973.** Elements of photogrammetry, Parts I & II. Department of Geodetic Science, Publications of The Ohio State University, Columbus, Ohio.

**Mikhail, E. 1976.** Observations and least squares. Harper & Row, New York.

**Moffitt, F. & Mikhail, E. 1980.** Photogrammetry. Harper & Row, New York.

**Nasr, A. 1983.** Effect of refinements of photo coordinates on the accuracy of transformation parameters. M.Sc. Thesis, Faculty of Engineering, Cairo University.

**Wolf, P. 1983.** Elements of photogrammetry. McGraw-Hill, New York.

*(Received 13 October 1984, revised 2 November 1985)*

# تأثير تصحيحات احداثيات الصور على دقة عناصر التقاطع والتوجيهات للصورة الواحدة

محمد شوقي الغزالي
قسم الهندسة المدنية
بجامعة الكويت

أشرف نصر سيد
قسم الهندسة المدنية
بكلية الهندسة ، جامعة القاهرة ،
الجيزة ، ج . م . ع

## خلاصة

في الفوتوجرامتري يعتمد الشرط الخطي على فرض ان النقطة في الجسم الذي يتم تصويره والنقطة التي تمثل محطة التصوير الجوي (مركز العدسة) والنقطة المناظرة على الصورة تقع جميعها على خط مستقيم واحد . لكن من الناحية العملية نجد ان هذا الخط المستقيم يحدث له انحراف ناتج عن سلسلة من الاخطاء المنتظمة الخطية وغير الخطية مما يؤدي الى تغيير مواقع النقط على الصورة الجوية . تبحث هذه الدراسة في تأثير بعض مصادر الاخطاء الهامة على دقة تعيين عناصر التقاطع والتوجيهات بالنسبة للصورة الواحدة . وقد وجد انه عند تصويب هذه الاخطاء على احداثيات الصور فان متوسط اخطاء الارصاد المتبقية بعد عملية الضبط بواسطة طريقة اقل مجموع المربعات قد انخفض من ٨ ميكرون الى ٦ ميكرون بالنسبة لمقياس رسم الصورة الجوية . كما تم توضيح ان تصويب الخطأ الناتج عن انكسار الاشعة خلال مرورها في طبقات الجو والخطأ الناشيء عن كروية الارض يجب ان يطبقا معا أو يهملا معا نظرا لانهما يعادلان بعضهما الى حد كبير . وفي الحقيقة فان تصويب احدهما دون الاخر يؤدي الى تدهور في دقة تعيين العناصر .